Optimal Charging and Discharging Operation of Mobile Charging Stations

Abdullah Kürşat Aktar
Electrical Electronics Engineering Dept.
Muğla Sıtkı Koçman University
Muğla, Turkey
kursataktar@mu.edu.tr

Akın Taşcıkaraoğlu
Electrical Electronics Engineering Dept.
Muğla Sıtkı Koçman University
Muğla, Turkey
akintascikaraoglu@mu.edu.tr

João P. S. Catalão
Faculty of Engineering of the
University of Porto and INESC TEC
Porto, Portugal
catalao@fe.up.pt

2022 International Conference on Smart Energy Systems and Technologies (SEST) | 978-1-6654-0557-7/22/$31.00 ©2022 IEEE | DOI: 10.1109/SEST53650.2022.9898463

***Abstract*—Today's technologies continue to grow by merging many various fields. The collaboration between electrical, electronic, mechanical and information technology is a necessity to re-evaluate the electrical energy system for including electric vehicles (EVs). In this study, the use of mobile charging stations (MCSs), which is expected to be one of the important components of the future energy systems, is considered to improve the satisfaction of EV users and an optimization algorithm is proposed to use MCS to minimize the quantity of the EVs that were not served. The results show that the use of MCS provides both operational and economic benefits compared to the expansion of permanent charging stations (PCSs) for increasing charging demands.**

***Index Terms*—Electric vehicle, energy storage, mobile charging station, vehicle-to-vehicle charging.**

I. Introduction

The increase in the world population, technological developments and environmental concerns force the energy sector to change at a macro level. One of the major changes is the electrification of vehicles in the transport sector. By 2030, it is estimated that there will be more than 110 million electric vehicles (EVs) worldwide and these EVs will demand a total energy of 500 TWh [1]. Moreover, the energy demand of the transportation sector will reach 11% of the global demand by 2040 [1].

The proliferation of decentralized energy systems and increase in the number of prosumers necessitate advanced management systems in electrical power systems. Considering the diversity of instruments in the system, it is obvious that it would not be sufficient to meet the demand simply by establishing more centralized power plants. There is a need to optimally manage such a large system by using different technologies such as bidirectional EV energy flows, demand side management strategies and EV charging stations, and by making use of information technologies [2].

Today's power systems include EVs, renewable energy sources, energy storage systems, energy markets with various price mechanisms and smart homes. It is possible to operate this system more efficiently if the data collected from all instruments of the system are processed effectively [3]. By doing so, all the system stakeholders can gain significant economic advantages. While the distribution system operator controls the peak energy period, the energy demand becomes more flexible with the incentives given to the consumers. Additionally, in terms of the commitments made by the countries in the climate agreement, it will create an opportunity for political executives [4].

In a decentralized system, many consumers can have their own power production units and EV charging facilities, and equip them with smart home devices to gain economic benefits if it is allowed by system operators. Besides, storing the energy produced by different energy sources and shifting some flexible loads from the peak energy period to a different time might provide significant economic benefits to consumers [5]. Also, private companies and electrical system operators develop their own solutions in order to provide a more reliable service.

Mobile charging stations (MCSs), which can be easily dispatched according to the energy demand for charging, stand out in terms of providing fast solutions and preventing very high investments [6]. It is possible to serve alongside the fixed charging stations during peak energy periods, and it is also possible to provide energy in suitable areas in off-grid mode [7]. Moreover, instead of deciding the location of mobile charging operations according to the regional charge service demand, it could be possible to provide safe charging services to EV users anywhere with IoT-based applications [8]. Among the studies for mobile charging, in [9] it was aimed to place the minimum number of MCS for both safe and economical management of the system operator, while in [10] and [11] additional MCS capacity was defined to reduce the waiting times of EV users. From a different perspective, the effect of MCS on reactive power capability and voltage quality was investigated in [12]. Also, the challenges in various areas, such as financial, battery life, energy transfer efficiency, socket types and wireless energy transfer were reviewed in detail in [13].

In this study, a distribution system with different types of consumers, medium-scale wind and biomass energy power plants, permanent charging stations (PCSs) and a MCS that is capable of providing bidirectional energy flow is considered. In the system, the MCS is a self-powered EV and has charging sockets on it. It is considered that the MCS can behave as an energy storage system for supporting the EV load demand during the peak energy period. While the MCS can be charged at several different points of the considered distribution system, it can only serve for discharging at a limited number of points. In the determination of these points, the routing constraints such as MCSs' travel time between buses are taken into account. The contributions of this study are threefold:

- The developed energy management algorithm examines the role of MCSs in facilitating the operation of the grid and reducing the number of EVs waiting for charging.
- Both energy storage and charging features of MCSs are evaluated within the scope of Vehicle-to-Vehicle (V2V).
- The obtained results provide an insight into the real applications of MCSs and V2V technology.

The paper consists of four sections. In Section II, the designed system is duly explained. The constrained optimization algorithm is evaluated for different situations in Section III and lastly the conclusion and possible future studies are included in Section IV.

978-1-6654-0557-7/22/$31.00 ©2022 IEEE

TABLE I. SETS

B_l^{ij}	Index of sending end i buses and receiving end j buses.
i	Index of buses.
l	Index of lines.
t	Index of time interval for energy flow.
tt	Index of time interval for travel of MCS.
v	Index of MCS velocity.

TABLE II. PARAMETERS

A	MCS Vehicle frontal area [m^2].
B_l	Susceptance of line l [pu].
C_d	Aerodynamic drag coefficient.
C_{rr}	Coefficient of rolling resistance.
CE^{MCS}	Charging efficiency of the MCS battery [%].
CS^{MCS}	Number of charging and discharging socket of MCS.
CS^{PCS}	Number of charging and discharging socket of PCS.
DE^{MCS}	Discharging efficiency of the MCS battery [%].
EC^{MCS}	Energy consumption of MCS [W].
$F_{v,tt}^{a}$	Aerodynamic drag force of MCS in time interval tt [pu].
$F_{v,tt}^{ac}$	Acceleration force of MCS in time interval tt [pu].
F_{tt}^{g}	Gravity force of MCS in time interval tt [pu].
F_{tt}^{r}	Rolling friction force of MCS in time interval tt [pu].
$F_{v,tt}^{t}$	Total traction force of MCS in time interval tt [pu].
f_m	Mass factor.
g	Gravity of earth [m/s^2].
M^{MCS}	Mass of MCS [kg].
$M_{i,l}^{F}$	Coefficient is 1 if line l of bus i is receiving end; 0 if line l of bus i is sending end; 0 if it is not both.
$M_{i,l}^{L}$	Coefficient is 1 if line l of bus i is sending end; 0 if it is not.
$M_{l,i}^{W}$	Coefficient that belongs to bus i and line l is obtained from transpose of $M_{i,l}^{F}$ matrix.
$P_{v,tt}^{ve}$	Electrical power demand of MCS in time interval tt [W].
$P_{v,tt}^{vm}$	Mechanical power demand of MCS in time interval tt [W].
$P_{i,t}^{L,total}$	Active power demand of bus i in time interval t [pu].
$Price_t$	Electricity price in time interval t [€/kWh].
$P_{i,t}^{CPD}$	Charging power demand of bus i in time interval t [pu].
$P_{i,t}^{W}$	Active power generation by wind farm at bus i in time interval t [pu].
$P_{i,t}^{BM}$	Active power generation by biomass power plant at bus i in time interval t [pu].
$Q_{i,t}^{L}$	Reactive power demand of bus i in time interval t [pu].
$R_i^{MCS,\mathrm{ch}}$	Charging rate limit of MCS that is connected bus i [pu].
$R_i^{MCS,dis}$	Discharging rate limit of MCS that is connected bus i [pu].
$R_i^{PCS,PD}$	Discharging rate limit of PCS that is connected bus i [pu].
R_l	Resistance of line l [pu].
$SOE^{MCS,ini}$	Initial SOE of the MCS [pu].
$SOE^{MCS,max}$	Maximum SOE of the MCS [pu].
$SOE^{MCS,min}$	Minimum SOE of the MCS [pu].
$T_{i,j}$	MCS travel time interval t from bus i to bus j.
TR^{lim}	Power limit of transformer [pu].
V_{max}	Permitted maximum voltage level of buses [pu].
V_{min}	Permitted minimum voltage level of buses [pu].
$V_{v,tt}^{MCS}$	MCS vehicle speed [m/s].
$V_{v,tt}^{W}$	Wind speed [m/s].
X_l	Reactance of line l [pu].
α	Acceleration [m^2/s].
η_d	Driving efficiency.
ρ	Air density [kg/m^3].
θ	Road slope angle [°].
ΔT	Time period [min].

TABLE III. VARIABLES

$m1_{i,t}$	Binary variable (1 if the MCS is connected bus i in time interval t; 0 otherwise).
$m2_t$	Binary variable (1 if the MCS is on travel in time interval t; 0 otherwise).
$m3_{i,t}$	Binary variable (1 if the MCS leaves the bus i during time interval t; 0 otherwise).
$m4_{i,t}$	Binary variable (1 if the MCS is connected to the bus i during time interval t; 0 otherwise).
$P_{i,t}^{G}$	Total active power of bus i in time interval t [pu].
$P_{i,t}^{L}$	Total power demand of bus i in time interval t [pu].
$P_{i,t}^{S}$	Total power flowing from transformer to bus i in time interval t [pu].
$P_{i,t}^{MCS,ch}$	Charging power by MCS that is connected bus i in time interval t [pu].
$P_{i,t}^{MCS,dis}$	Discharging power by MCS that is connected bus i in time interval t [pu].
$P_{i,t}^{PCS,PD}$	Charging power by PCS to charge EVs in the queue at bus i in time interval t [pu].
$P_{l,t}^{\mathrm{loss}}$	Total active power loss of line l in time interval t [pu].
$\hat{P}_{l,t}^{\mathrm{loss}}$	Model variable to represent total active power loss of line l in time interval t [pu].
$P_{l,t}^{r}$	Total active power of line l in time interval t [pu].
$Q_{l,t}^{\mathrm{loss}}$	Total reactive power loss of line l in time interval t [pu].
$Q_{i,t}^{G}$	Total reactive power of bus i in time interval t [pu].
$Q_{i,t}^{r}$	Total reactive power of line l in time interval t [pu].
SOE_t^{MCS}	SOE of the MCS battery in time interval t [pu].
$u_{i,t}^{ch}$	Binary variable (1 if the MCS is charging in time interval t; 0 otherwise).
$u_{i,t}^{dch}$	Binary variable (1 if the MCS is discharging in time interval t; 0 otherwise).
$V_{i,t}$	Voltage magnitude of bus i in time interval t [pu].
$W_{i,t}$	Equivalent of cosine term of power flow equation on line (i,j) in time interval t [pu].
$W_{r,t}$	Square of voltage magnitude at receiving end bus r ($r \in i$) in time interval t [pu].

II. METHODOLOGY

A distribution system with 15 buses with different load characteristics is considered in this study. Two PCSs connected to the buses of the distribution system and one MCS that can be charged from different nodes in the system are placed. All the PCSs and MCSs are considered as the assets of the distribution system operator and are used to charge the EVs while also providing economic benefits and improving the power system reliability. The MCS settles in the PCS area at the required time intervals and performs V2V operations with its charging sockets without connecting to the grid. The load demand is met by the transformer in the system and the energy generation of the wind farm and biomass power plant contributes to the system. Distribution system diagram with the power plants and MCS charge/discharge buses are shown in Fig. 1. The designed system aims to make the optimum use of the MCS and the charging station aspects of EVs that are used for V2V operations. The objective function, constraints of the system and other expressions are given by Eqs. (1)-(31).

The proposed approach aims to maximize the operational and economic benefits of MCSs by using them as mobile energy storage and charging systems. The main purpose of the proposed constrained optimization algorithm is to minimize the difference between the total hourly power demand of EVs and the power supplied by PCS and MCS, as shown in Eq. (1). Thus, the number of missed vehicles is determined by dividing the minimized amount of power by the rated power of a socket. Eqs. (2) and (3) show active and reactive energy flow relations. As stated in Eqs. (4) and (5), the transformer, wind farm and biomass power plant constitute the supplier part in the system, while commercial, domestic and EV charging load form the consumer part. AC power flow equations taken from [14] are given in Eqs. (6)-(11). These equations presented in a second-order cone formulation can be used in a linear optimization algorithm by choosing the appropriate solver. MCS charging and discharging power constraints are shown by (12) and (13), respectively. Eq. (14) prevents simultaneous charging and discharging in time interval t when the MCS is connected to bus i. The PCS has unidirectional energy flow and Eq. (15) specifies the power flow constraint for EV charging. Calculation of the MCS's battery state-of-the-energy (SOE) according to the operation mode of charge, discharge or travel is done by Eq. (16). Battery capacity constraints and initial value are defined by Eqs. (17) and (18), respectively.

$$Minimize\ MV = \sum_t \sum_i ((P_{i,t}^{CPD} - P_{i,t}^{MCS,dis} - P_{i,t}^{PCS,PD}) \cdot \Delta T) \quad (1)$$

subject to:

$$P_{i,t}^G - P_{i,t}^L = \sum_{l \in B_l^{ij}} \left(M_{i,l}^F \cdot P_{l,t}^r + M_{i,l}^L \cdot P_{l,t}^{\text{loss}} \right) \ \forall i,t \quad (2)$$

$$Q_{i,t}^G - Q_{i,t}^L = \sum_{l \in B_l^{ij}} \left(M_{i,l}^F \cdot Q_{l,t}^r + M_{i,l}^L \cdot Q_{l,t}^{\text{loss}} - B_l \cdot M_{l,i}^W \cdot W_{i,t} \right) \ \forall i,t \quad (3)$$

$$P_{i,t}^G = P_{i,t}^S + P_{i,t}^W + P_{i,t}^{BM} \ \forall i,t \quad (4)$$

$$P_{i,t}^L = P_{i,t}^{L,total} + P_{i,t}^{MCS,\text{ch}} + P_{i,t}^{PCS,PD} \ \forall i,t \quad (5)$$

$$W_{i,t} = V_{i,t}^2 \ \forall i,t \quad (6)$$

$$P_{l,t}^{\text{loss}} = 2 \cdot R_l \cdot \hat{P}_{l,t}^{\text{loss}} \ \forall l,t \quad (7)$$

$$X_l \cdot P_{l,t}^{\text{loss}} - R_l \cdot Q_{l,t}^{\text{loss}} = 0 \ \forall l,t \quad (8)$$

$$\sum_i \left(M_{l,i}^W \cdot W_{i,t} \right) - 2 \cdot \left(R_l \cdot P_{l,t}^r + X_l \cdot Q_{l,t}^r \right) = R_l \cdot P_{l,t}^{\text{loss}} + X_l \cdot Q_{l,t}^{\text{loss}} \ \forall l,t \quad (9)$$

$$2 \cdot \hat{P}_{l,t}^{loss} \cdot W_{r,t} \geq {P_{l,t}^r}^2 + {Q_{l,t}^r}^2 \ \forall l,t \quad (10)$$

$$V_{min}^2 \leq W_{i,t} \leq V_{max}^2 \ \forall i,t \quad (11)$$

$$0 \leq P_{i,t}^{MCS,\text{ch}} \leq R_i^{MCS,\text{ch}} \cdot u_{i,t}^{ch} \ \forall i,t \quad (12)$$

$$0 \leq P_{i,t}^{MCS,dis} \leq R_i^{MCS,dis} \cdot u_{i,t}^{dch} \ \forall i,t \quad (13)$$

$$u_{i,t}^{ch} + u_{i,t}^{dch} = m1_{i,t} \quad (14)$$

$$0 \leq P_{i,t}^{PCS,PD} \leq R_i^{PCS,PD} \ \forall i,t \quad (15)$$

$$\text{SOE}_t^{\text{MCS}} = \text{SOE}_{(t-1)}^{\text{MCS}} + \sum_i \left(\text{CE}^{\text{MCS}} \cdot \text{P}_{\text{i,t}}^{\text{MCS,ch}} - \frac{\text{P}_{\text{i,t}}^{\text{MCS,dis}}}{\text{DE}^{\text{MCS}}} \right) \cdot \Delta T - (\text{EC}^{\text{MCS}} \cdot m2_t) \ \forall \text{t} \quad (16)$$

$$SOE^{MCS,min} \leq SOE_t^{MCS} \leq SOE^{MCS,max} \ \forall t \quad (17)$$

$$SOE_t^{MCS} = SOE^{MCS,ini} \ \ if\ t = 1 \quad (18)$$

$$\sum_i m1_{i,t} \leq 1 \ \forall t \quad (19)$$

$$m2_t = 1 - \sum_i m1_{i,t} \ \forall t \quad (20)$$

$$\sum_{t-T_{i,j}+1}^{t} m4_{i,t} \leq 1 - m3_{j,t} \ \forall t,i,j \quad (21)$$

$$m3_{j,t} - m4_{i,t} = m1_{i,t} - m1_{i,(t-1)} \ \forall i,t \quad (22)$$

$$m3_{j,t} + m4_{i,t} \leq 1 \ \forall i,t \quad (23)$$

$$F_{v,tt}^t = F_{v,tt}^{ac} + F_{v,tt}^a + F_{tt}^r + F_{tt}^g \ \forall v,tt \quad (24)$$

$$F_{v,tt}^a = \frac{1}{2} . \rho . A . C_d . (V_{v,tt}^{MCS} - V_{v,tt}^W)^2 \ \forall v,tt \quad (25)$$

$$F_{tt}^r = M^{MCS} . g . C_{rr} . \cos(\theta) \ \forall tt \quad (26)$$

$$F_{tt}^g = M^{MCS} . g . \sin(\theta) \ \forall tt \quad (27)$$

$$F_{v,tt}^{ac} = f_m . M^{MCS} . \alpha \ \forall v,tt \quad (28)$$

$$P_{v,tt}^{vm} = F_{v,tt}^t . V_{v,tt}^{MCS} \ \forall tt \quad (29)$$

$$P_{v,tt}^{ve} = \frac{P_{v,tt}^{vm}}{\eta_d} \ \forall tt \quad (30)$$

$$EC^{MCS} = \sum_{tt} \left(P_{v,tt}^{ve} . \Delta T \right) \quad (31)$$

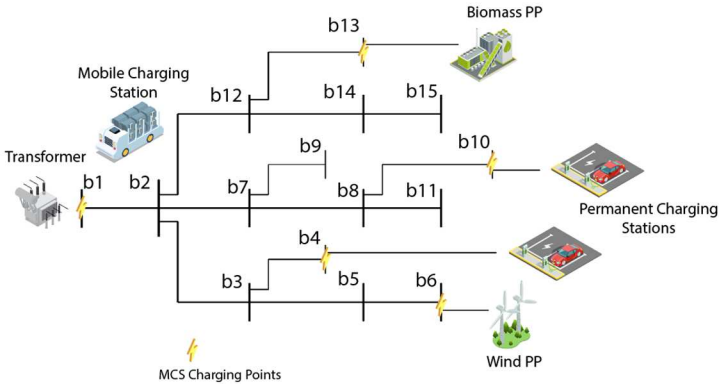

Figure 1. Block diagram of the system considered.

Connection and routing constraints of MCS are given by Eqs. (19)–(23). Eq. (19) ensures that the MCS can only be connected to one bus node in a time interval. If the MCS is not connected to any bus in time interval t, its traveling condition is expressed by Eq. (20). However, the MCS traveling from the bus i to the bus j is prevented from connecting to the bus j before the required travel time has elapsed by Eq. (21). The change in the arrival and departure status and preventing the MCS from arriving at a bus node and leaving at the same time are expressed in (21) and (22), respectively. The energy consumption of the MCS is calculated according to Eqs. (24)-(31) that are taken from [15]. Four main forces, which are the acceleration force, $F_{v,tt}^{ac}$, aerodynamic drag force, $F_{v,tt}^a$, rolling friction force, F_{tt}^r, and gravity force, F_{tt}^g constitute the total traction force $F_{v,tt}^t$. Eqs. (29) and (30) are used to calculate the mechanical and electrical power needed, respectively. Total energy consumption of MCS to travel between two bus nodes is calculated by Eq. (31).

III. Results and Discussion

A. Input Data

The data of the 15-bus distribution system are shown in Table IV [16]. Resistance and reactance values are expressed as per unit. In addition, a base voltage of 12.66 kV, a base apparent power of 100 kVA and a base impedance of 1602 Ω are used.

During the displacement of any EV, an energy consumption occurs depending on the parameters related to the EV and environment. MCS moves between bus nodes in different locations to provide the most optimum service. The values used to calculate the energy consumption during the travel of the MCS are shown in Table V. A single type of EV is utilized in the study; however, the consumption values of different EVs and various environmental conditions can be included with minor changes. Moreover, the change in the SOE of the MCS appears while charging from grid and discharging to serve EVs. Parameters regulating charging and discharging operations are given in Table VI. The load demand of the consumers, the generated power values of the wind farm and biomass power plant are considered for a period of one day in the study, as shown in Fig. 2.

According to the designed system, while MCS can be charged at five different bus nodes, it provides discharge service at only 2 nodes that are PCS areas. Available points for charging and discharging are indicated in Fig. 1. Another important issue that the optimization algorithm considers while making a decision is the socket number and priority order of the MCS and PCS. In the study, while MCS has 18 sockets, each PCS has 10 sockets.

By taking into account the number of EVs arriving at the charging points, the optimization algorithm determines the point where MCS will provide the most appropriate service and gives priority to the sockets of the MCS. If there are EVs waiting after the MCS switches to full capacity operation, the sockets of the PCS are activated.

The EV queue graph used in making the service point decision of the MCS is shown in Fig 3, and the graph showing the time periods required for the MCS to travel between bus nodes is shown in Table VII.

B. Simulation and Results

In order to reveal the benefits of the proposed approach, three different cases are evaluated:

- **Case 1:** MCS is movable and energy tariff is fixed pricing.
- **Case 2:** MCS is fixed at Bus 10 and energy tariff is fixed pricing.
- **Case 3:** MCS is movable and energy tariff is dynamic pricing.

A time granularity of one hour is used in all three cases. -In Case 1, the MCS operates in optimum conditions according to the demand in the charging areas in a system where energy prices are fixed. In addition, instead of an increase in the socket number of PCSs which are busy for a period of the day, the benefits of using MCS are investigated. Moreover, it could be useful as a quick and simple solution where grid infrastructure is not suitable to extend. -In Case 2, it is assumed that the MCS is connected to Bus 10 and never disconnected during the test period. In the two cases mentioned above, the optimization algorithm aims to minimize the number of EVs that cannot be served as there are no empty sockets. -In Case 3, the status where the MCS is movable and prices are varying on an hourly basis is evaluated. For this purpose, with a change made in the objective function, both the number of EVs that cannot be served and energy costs are minimized.

TABLE IV. LINE PARAMETERS OF THE DISTRIBUTION SYSTEM

Line	From	To	R[pu]	X[pu]	Line	From	To	R[pu]	X[pu]
L1	1	2	0	0	L8	7	9	0.11	0.11
L2	2	3	0.075	0.1	L9	8	10	0.11	0.11
L3	3	4	0.08	0.11	L10	8	11	0.08	0.11
L4	3	5	0.09	0.18	L11	2	12	0.11	0.11
L5	5	6	0.04	0.04	L12	12	13	0.09	0.12
L6	2	7	0.11	0.11	L13	12	14	0.08	0.11
L7	7	8	0.08	0.11	L14	14	15	0.04	0.04

TABLE V. MCS AND ENVIRONMENTAL PARAMETERS TO CALCULATE ENERGY CONSUMPTION

Parameter	Value	Parameter	Value
Coefficient of rolling resistance	0.02	Aerodynamic drag coefficient	0.5
Mass	5000 kg	Wind speed	0 m/s
Mass factor	1.05	Road slope angle	0 °
Air density	1.225 kg/m^3	Gravity of Earth	9.8 m/s^2
Vehicle frontal area	4 m^2	Efficiency of MCS	0.9

TABLE VI. MCS PARAMETERS FOR ENERGY EXCHANGE

Parameter	MCS	PCS	Parameter	MCS	PCS
CE^{MCS}	0.95	-	$SOE^{MCS,ini}$	200 kWh	-
DE^{MCS}	0.95	-	$SOE^{MCS,min}$	200 kWh	-
$R^{MCS/PCS,ch}$	20 kW/socket	20 kW/socket	$SOE^{MCS,max}$	2500 kWh	-
$R^{MCS/PCS,dis}$	20 kW/socket	20 kW/socket			

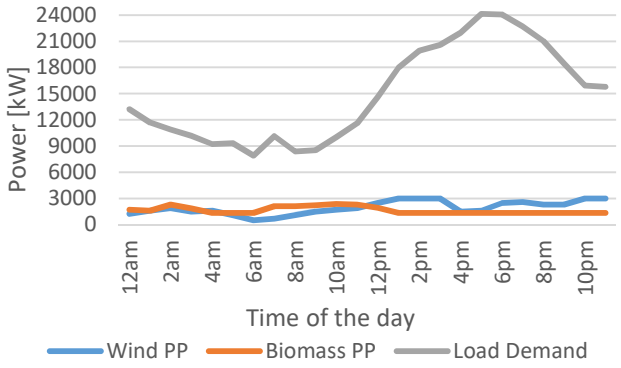

Figure 2. The power demanded and energy generation of power plants during the test period.

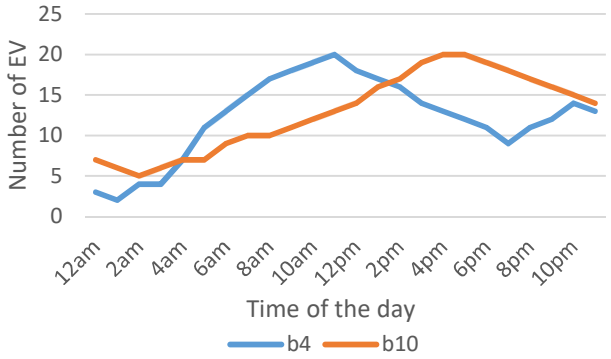

Figure 3. The number of EVs waiting for charge at Bus 4 and Bus 10.

TABLE VII. REQUIRED TRAVEL TIME BETWEEN BUS NODES

Road	From [Bus]	To [Bus]	Period [t]	Road	From [Bus]	To [Bus]	Period [t]
R1	B1	B4	2	R6	B4	B10	3
R2	B1	B6	1	R7	B4	B13	2
R3	B1	B10	1	R8	B6	B10	2
R4	B1	B13	1	R9	B6	B13	2
R5	B4	B6	3	R10	B10	B13	2

As shown in Fig. 4, the MCS battery completes the test period with its initial SOE by performing the charge and discharge operations at different time intervals. Bus nodes where MCS performs these operations are indicated in Fig. 5.

After determining the use of the limited charging sockets of MCS, the number of EVs that could not be serviced in the relevant buses is shown in Fig. 6. On the other hand, the comparison of the number of active sockets in PCS and MCS, the number of EVs that coming to charge and the number of EVs that could not be charged are given in Fig. 7.

Expansions in the PCS can be made in order to reduce the charge demand congestion that occurs especially at certain times of the day. Based on this fact, in Case 2, the MCS is fixed to Bus 10 as shown in Fig. 9. In this operating mode, where it acts as an energy storage system, the characteristic curves of the battery could be seen in Fig. 8. In this case, it is seen from Fig. 10 that it carries out the charging and discharging operations in the connected bus nodes in a way that reduces the missing EVs. As can be seen from the outputs in Fig. 11, the fixed MCS operation is less efficient compared to the mobile operation (shown in Fig. 7).

In Case 3, differently from the previous cases, energy prices have dynamic characteristic on an hourly basis. To this end, a change is made in the objective function as seen in (32).

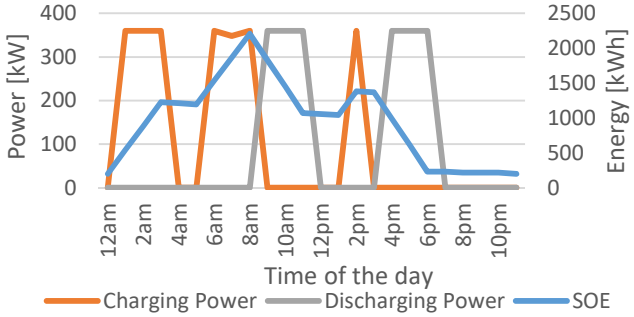

Figure 4. Battery outputs of MCS for Case 1.

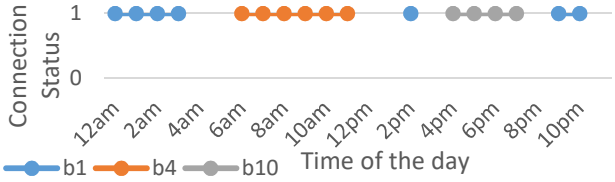

Figure 5. MCS connection status during the test period for Case 1.

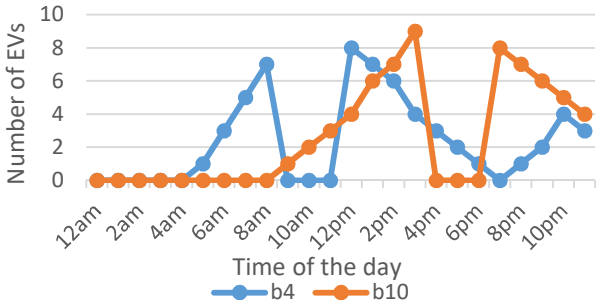

Figure 6. Number of EVs missed due to lack of sockets for Case 1.

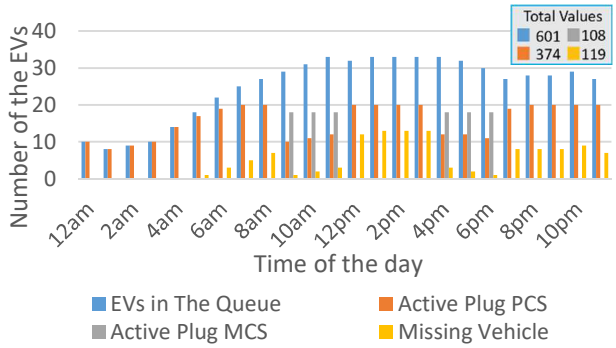

Figure 7. Comparison of the PCS, MCS, EV queue and missing EV for Case 1.

The increase in energy prices with load demand, shown in Fig. 12, highlights the value of MCS's mobile battery feature. Thanks to this feature, economic benefits are provided by charging when electricity prices are lower and discharging when electricity is more expensive. At the same time, the objective function aims to minimize the number of missed EVs. Thus, a multi objective situation arises in terms of both electrical grid and charging operation. It is seen from the MCS battery characteristic shown in Fig. 13 that the charging operation takes place in the cheaper price period, and discharge occurs when both prices and number of EVs coming to charge are high.

Besides, Fig. 14 shows that MCS is in operation at Bus 1, Bus 4 and Bus 10 during the test period. The discharge operation takes place between 3:00 pm and 7:00 pm, which is the peak period of the price and charging orders as seen in Fig. 15. Statistical outputs of MCS and PCS are given in Fig. 16.

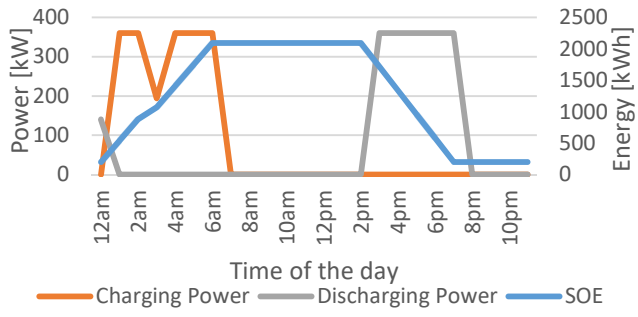

Figure 8. Battery outputs of MCS for Case 2.

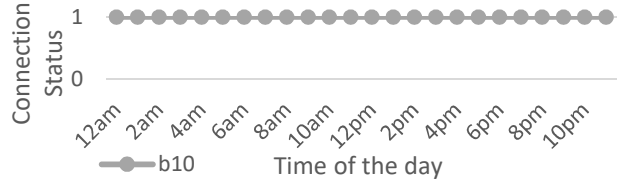

Figure 9. MCS connection status during the test period for Case 2.

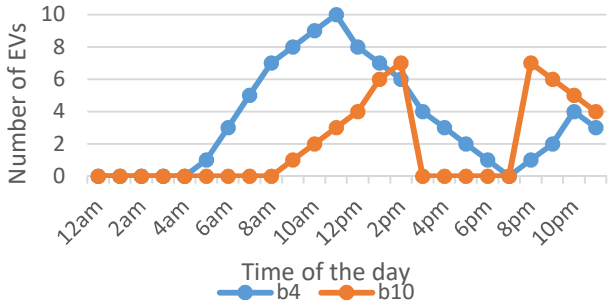

Figure 10. Number of EVs missed due to lack of sockets for Case 2.

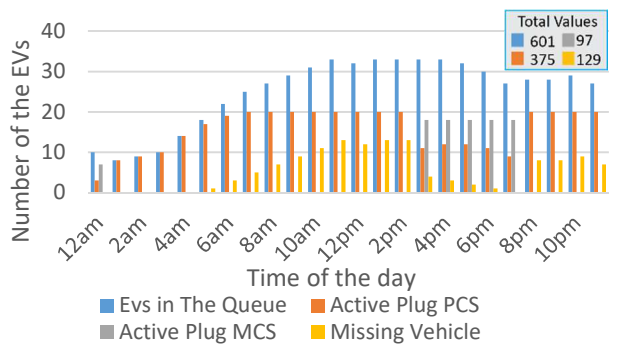

Figure 11. Comparison of the PCS, MCS, EV queue and missing EV for Case 2.

$$Minimize\ MV = \sum_t \sum_i ((P_{i,t}^{CPD} - P_{i,t}^{MCS,dis} - P_{i,t}^{PCS,PD}) \cdot \Delta T \cdot Price_t) + \sum_t \sum_i ((P_{i,t}^{MCS,ch} - P_{i,t}^{MCS,dis}) \cdot \Delta T \cdot Price_t) \quad (32)$$

Lastly, regarding the number of EVs that could not be serviced for all cases, in Case 2, since the MCS is fixed to Bus 10, it only serves the relevant bus. Therefore, 129 EVs are not charged for Case 2 when evaluated for the entire test period.

Similarly, when Case 1 and Case 3 are evaluated, it is calculated that 119 and 120 EVs are not served, respectively. In Case 1, where the prices do not change and the MCS is movable, it is seen that the least number of EVs are missed. Likewise, as the MCS is fixed on Bus 10, which is busy in a very short time of the day, it turns out that Case 2 is the most missed EV case.

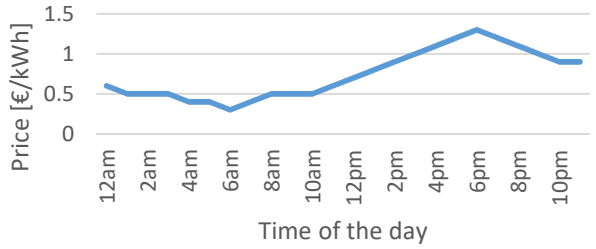

Figure 12. Dynamic electricity price for Case 3.

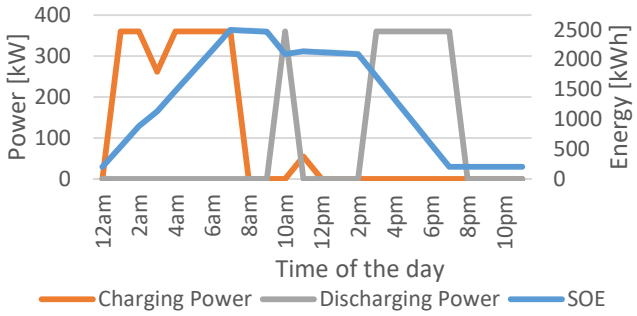

Figure 13. Battery outputs of MCS for Case 3.

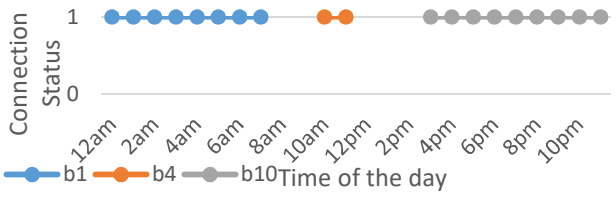

Figure 14. MCS connection status during the test period for Case 3.

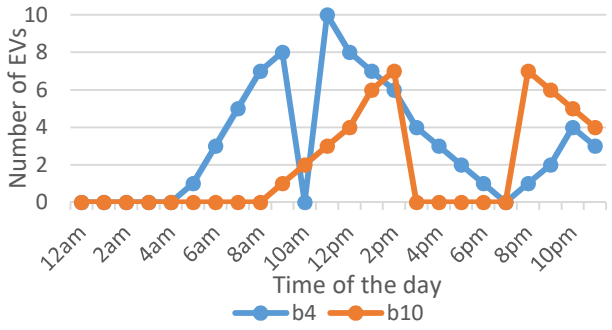

Figure 15. Number of EVs missed due to lack of sockets for Case 3.

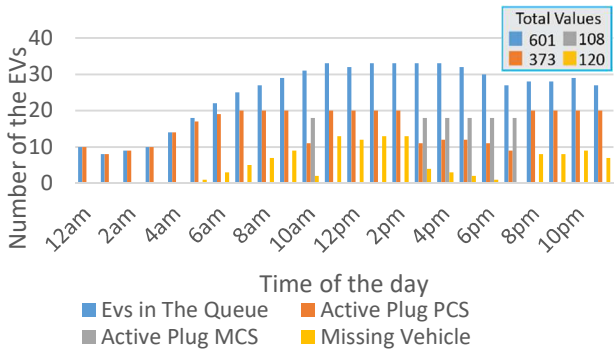

Figure 16. Comparison of the PCS, MCS, EV queue and missing EV for Case 3.

IV. Conclusions and Future Work

The constrained optimization algorithm is aiming at using an MCS as a mobile energy storage system and charging station at appropriate buses to supply to the highest number of EVs while providing effective grid management. The results demonstrated that using MCS was beneficial in reducing the number of EVs waiting for charging at different buses at different time intervals. In addition, fixing the MCS to a single point did not provide a significant advantage in terms of operation. However, it might be useful where the grid infrastructure is inadequate. In the networks where the electricity prices are dynamic, when the right energy storage capacity is chosen, it may be possible to increase both the economic and operational benefits in the peak energy period. As a future study, the role of renewable energy sources in the system can be increased by considering different numbers of MCS and charging load demand. Besides, MCS's purchasing, maintenance, repair and battery degradation costs might be included in the optimization algorithm.

Acknowledgment

This work of A. Taşcıkaraoğlu is supported by the Turkish Academy of Sciences (TUBA) within the framework of the Distinguished Young Scientist Award Program (GEBIP).

References

[1] L. Cozzi et al., "World Energy Outlook 2020," vol. 2050, no. October, pp. 1–461, 2020

[2] A. Alsharif, C. W. Tan, R. Ayop, A. Dobi, and K. Y. Lau, "A comprehensive review of energy management strategy in Vehicle-to-Grid technology integrated with renewable energy sources," *Sustain. Energy Technol. Assessments*, vol. 47, no. June, p. 101439, 2021.

[3] O. Ouramdane, E. Elbouchikhi, Y. Amirat, and E. S. Gooya, "Optimal sizing and energy management of microgrids with Vehicle-to-Grid technology: A critical review and future trends," *Energies*, vol. 14, no. 14, 2021.

[4] N. K. Panda and N. G. Paterakis, "A multi-objective optimization model for the quantification of flexibility in a large business park," *SEST 2021 - 4th Int. Conf. Smart Energy Syst. Technol.*, 2021.

[5] S. Taik, J. Guo, B. Kiss, and I. Harmati, "Demand Response of Multiple Households with Coordinated distributed Energy Resources," *2021 25th Int. Conf. Methods Model. Autom. Robot.* MMAR 2021, pp. 203–208, 2021.

[6] S. Afshar, P. Macedo, F. Mohamed, and V. Disfani, "Mobile charging stations for electric vehicles — A review," *Renew. Sustain. Energy Rev.*, vol. 152, no. July 2020, p. 111654, 2021.

[7] H. Saboori, S. Jadid, and M. Savaghebi, "Optimal management of mobile battery energy storage as a self-driving, self-powered and movable charging station to promote electric vehicle adoption," *Energies*, vol. 14, no. 3, 2021.

[8] H. Chen, Y. Zhao, R. Zhang, Z. Chen, and S. Chen, "Optimal Security Charging Service for Electric Vehicles by Mobile Charging Stations: Dynamic Contract-based Approach," *2021 33rd Chinese Control and Decision Conference*, pp. 4627–4632, 2021.

[9] M. S. Raboaca, I. Bancescu, V. Preda, and N. Bizon, "An optimization model for the temporary locations of mobile charging stations," *Mathematics*, vol. 8, no. 3, pp. 1–20, 2020.

[10] V. Chauhan and A. Gupta, "Scheduling Mobile Charging Stations for Electric Vehicle Charging," *Int. Conf. Wirel. Mob. Comput. Netw. Commun.*, vol. 2018-October, pp. 131–136, 2018.

[11] I. El-Fedany, D. Kiouach, and R. Alaoui, "A Smart Coordination System Integrates MCS to Minimize EV Trip Duration and Manage the EV Charging, Mainly at Peak Times," *Int. J. Intell. Transp. Syst. Res.*, vol. 19, no. 3, pp. 496–509, 2021.

[12] S. Jeon and D. H. Choi, "Optimal energy management framework for truck-mounted mobile charging stations considering power distribution system operating conditions," *Sensors*, vol. 21, no. 8, 2021.

[13] S. Afshar, P. Macedo, F. Mohamed, and V. Disfani, "Mobile charging stations for electric vehicles — A review," *Renew. Sustain. Energy Rev.*, vol. 152, no. August, p. 111654, 2021.

[14] M. Baradar and M. R. Hesamzadeh, "AC power flow representation in conic format," *IEEE Trans. Power Syst.*, vol. 30, no. 1, pp. 546–547, 2015.

[15] J. A. P. L. Garcia-Val, Rodrigole, Ed., *Power Electronics and Power Systems*. Springer, 2013.

[16] A. K. Erenoğlu and O. Erdinç, "Post-Event restoration strategy for coupled distribution-transportation system utilizing spatiotemporal flexibility of mobile emergency generator and mobile energy storage system," *Electr. Power Syst. Res.*, vol. 199, no. March, 2021.